

Heat capacity of the quantum magnet TiOCl

J. Hemberger,^{1,*} M. Hoinkis,² M. Klemm,² M. Sing,² R. Claessen,^{2,†} S. Horn,² and A. Loidl¹

¹*Experimentalphysik V, Center for Electronic Correlations and Magnetism, Universität Augsburg, D-86135 Augsburg, Germany*

²*Experimentalphysik II, Institut für Physik, Universität Augsburg, D-86135 Augsburg, Germany*

(Received 21 January 2005; published 29 July 2005)

Measurements of the heat capacity $C(T, H)$ of the one-dimensional quantum magnet TiOCl are presented for temperatures $2 \text{ K} < T < 300 \text{ K}$ and magnetic fields up to 5 T. Distinct anomalies at 91 and 67 K signal two subsequent phase transitions. The lower of these transitions clearly is of first order and seems to be related to the spin degrees of freedom and the lattice. The transition at 91 K is of second order. A detailed analysis of the data reveals that the entropy change ΔS through both transitions is surprisingly small ($\sim 0.1 \text{ R}$), pointing towards the existence of strong fluctuations well into the nonordered high-temperature phase.

DOI: [10.1103/PhysRevB.72.012420](https://doi.org/10.1103/PhysRevB.72.012420)

PACS number(s): 71.30.+h, 72.80.Ga, 65.40.Ba

I. INTRODUCTION

The discovery of high- T_c superconductivity in the cuprates and of colossal magnetoresistance in manganite perovskites generated an enormous interest in transition-metal oxides (TMOs). TMOs are characterized by an intimate coupling of spin, charge, orbital, and lattice degrees of freedom, which is the origin of a number of complex and exotic ground states. The discovery of a number of new low-dimensional spin 1/2 quantum magnets was another result of this renewed interest. After the first experimental observation of a spin-Peierls scenario in the organic compound TTF-CuBDT (Ref. 1) more than 30 years ago, CuGeO₃ (Ref. 2) was the first inorganic spin-Peierls system. Another paramount example is NaV₂O₅ (Ref. 3), a spin ladder with mixed-valent vanadium ions undergoing a charge-ordering transition.⁴ Further interest in these low-dimensional quantum magnets comes from the fact that upon doping they may undergo metal-to-insulator transitions and possibly reveal superconductivity. During the last decade TiOCl has been a distinguished candidate for a resonating-valence-bond ground state⁵ and has emerged as a further quantum-spin magnet with a gapped ground state.^{5,6}

Titanium oxochloride was synthesized by Friedel and Guerin in 1876 (Ref. 7). A detailed report on growth and characterization was given by Schäfer *et al.*⁸ almost 50 years ago. TiOCl crystallizes in the orthorhombic FeOCl structure, consisting of TiO bilayers separated by Cl layers. In this structure every Ti is surrounded by four oxygen and two chlorine ions forming a distorted octahedron. Originally, based on an analysis of susceptibility data combined with band-structure calculations, it has been suggested that the t_{2g} orbitals are orbitally ordered, producing one-dimensional antiferromagnetic $S=1/2$ chains.⁶ The high-temperature magnetic susceptibility could well be described by a Bonner-Fisher type of behavior with an exchange constant $J=660 \text{ K}$. A sudden drop of the susceptibility almost to zero indicated the opening of a spin gap at $T_{c1}=67 \text{ K}$, while a further anomaly has been detected at $T_{c2}\approx 95 \text{ K}$ (Ref. 6). Electron spin resonance,⁹ infrared, and Raman spectroscopy,^{10,11} as well as NMR measurements,¹² substantiated these results and established a spin gap of the order of 430 K. The origin of the gap has been identified as due to a first-

order spin-Peierls transition at T_{c1} , as evidenced by the observation of Ti dimerization in temperature-dependent x-ray diffraction.¹³ The nature of a second transition at T_{c2} is still unclear. While a broadening of the NMR line shape into a wide continuum below T_{c2} has been attributed to a possible incommensurate (orbital) ordering,¹² no corresponding superlattice reflections could be observed in x-ray scattering,¹³ though there is some evidence for a structural symmetry lowering from the high-temperature phase. Recently, another scenario was proposed, which describes a sequence from an incommensurate spin-Peierls regime below T_{c2} towards a lock-in transition into a commensurate dimerized phase at T_{c1} (Ref. 14). Close to $T^*\approx 135 \text{ K}$ the opening of a spin pseudogap as detected in NMR (Ref. 12) and the onset of giant phonon anomalies in infrared and Raman spectroscopy¹¹ indicated the presence of strong spin fluctuations and a pronounced coupling to the lattice, respectively, for temperatures up to $T^*\approx 135 \text{ K}$.

Electronically, TiOCl is a Mott insulator with nominally trivalent Ti. Electronic structure calculations using the local-density approximation (LDA)+ U predict a Ti $3d_{xy}^1$ ground state,^{6,15} however, coupling to optical-phonon modes can lead to strong orbital fluctuations within the t_{2g} crystal-field multiplet. The importance of correlation effects has been elucidated in LDA+ dynamical mean-field theory (DMFT) (Refs. 16 and 17) studies.

In this brief experimental report we provide detailed measurements of the heat capacity of TiOCl to further unravel the nature of the two phase transitions.

II. EXPERIMENTAL DETAILS

Single crystals of TiOCl were prepared by chemical vapor transport from TiCl₃ and TiO₂ (Ref. 8). The samples have been characterized using x-ray diffraction, superconducting quantum interference device (SQUID), and electron spin resonance (ESR) measurements at X-band frequencies. The crystal symmetry was found to be orthorhombic with lattice parameters of $a=0.379 \text{ nm}$, $b=0.338 \text{ nm}$, and $c=0.803 \text{ nm}$. The magnetic properties were found to be in excellent agreement with published results.^{6,9} The heat-capacity measurements have been performed with a commercial physical

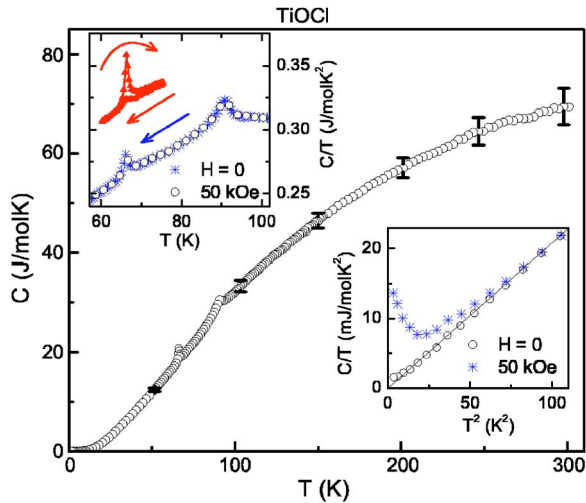


FIG. 1. (Color online) Heat capacity of TiOCl vs temperature. The vertical bars indicate experimental uncertainties and reveal the scatter of $C(T)$ in different measuring cycles with different temperature stimuli and using different samples. Upper inset: Magnified region of the two phase transitions. The heat capacity measured at 5 T (stars) is compared to the heat capacity in zero external field (circles), both measured on cooling: No significant difference between both curves can be detected. The temperature region around the lower transition at $T_{c1} \approx 66.7$ K was remeasured (triangles) utilizing a reduced relaxation amplitude of $\delta T \approx 0.5$ K on heating and subsequent cooling. For clarity these data are shifted by 50 mJ/mol K². Lower inset: Low-temperature heat capacity plotted as C/T vs T^2 . For the results in zero magnetic field a fit using a Debye-derived phonon contribution is indicated as a solid line.

properties measurement system (PPMS) from Quantum Design for temperatures $1.8 \text{ K} < T < 300 \text{ K}$ and in external magnetic fields up to 5 T.

III. RESULTS AND DISCUSSION

Figure 1 shows the central result of this investigation, the heat capacity as function of temperature. The heat capacity is characteristic for a three-dimensional solid with a Debye temperature of order 200 K. Superimposed, we find two weak but distinct anomalies which are clearly related to the two subsequent phase transitions at $T_{c1} = 67 \text{ K}$ and $T_{c2} = 91 \text{ K}$. In recent NMR experiments¹² slightly different temperatures, namely 94 and 66 K, respectively, have been determined. The effects of the phase transitions on the specific heat are remarkably weak and are almost lost under the large phonon-derived heat-capacity contributions, and it is clear that the entropy covered by the two anomalies is comparably small.

The upper inset in Fig. 1 shows the heat capacity (given as C/T vs T) in the temperature region of the phase transitions for both zero field and an external magnetic field of 5 T measured on cooling together with a special heating/cooling run in the vicinity of T_{c1} in zero field, which will be discussed later.

Concerning the magnetic-field dependence we observe no effects on the heat capacity within experimental uncer-

tainties. The moderate magnetic fields used here neither shift the transition temperatures, nor do they seem to affect the entropies involved in the phase transitions. On the other hand, the small energy of our fields of order $50 \text{ kOe} \times \mu_B$ ($\approx 0.06 \text{ meV}$) is negligibly small compared to the intrinsic magnetic energy scale of TiOCl as estimated from $k_B T_{c1,2}$ (5.8 and 7.9 meV) or the exchange constant J (57 meV).

In order to analyze the nature of the detected anomalies in terms of first- or second-order phase transitions, we performed heating/cooling cycles across the phase transitions. As the experimental setup utilizes a relaxation method, each data point is related to the average over a temperature interval above the initially stabilized temperature rather than to an exact temperature.¹⁸ This means that for the cooling sequence the temperature is decreased between the data acquisition and increased during the acquisition process itself. Thus, in the case of hysteretic (i.e., first-order) behavior, the actual transition, together with the corresponding release of latent heat, is fully captured only in the heating branch of the measuring sequence. Around T_{c1} a significant difference between heating and cooling can be detected, pointing towards a first-order transition (shifted curve in the inset of Fig. 1). No such feature could be found for the upper transition at T_{c2} .

The lower inset in Fig. 1 shows the low-temperature heat capacity plotted as C/T vs T^2 to search for possible spin contributions. In zero external magnetic field, $C(T)$ is fully determined by phonon contributions and from a linear fit (solid line) a Debye temperature of $\Theta'_D = 210 \text{ K}$ can be determined. The low-temperature heat capacity becomes slightly enhanced in magnetic fields of 5 T, which can be explained by the increasing importance of nuclear hyperfine contributions or the influence of paramagnetic defects at the lowest temperatures. For comparison, the low-temperature specific heat of the canonical organic spin-Peierls compound (TMTTF)₂PF₆ (Ref. 19) displays, besides the nuclear hyperfine and T^3 phonon contributions, an additional quasilinear ($\sim T^{1.2}$) term which has been ascribed to low-energy excitations. A similar contribution certainly can be excluded for TiOCl.

In the following analysis we will decompose the heat capacity into phonon and spin ($S=1/2$) contributions, with the former dominating the latter for all temperatures. Nevertheless, we are able to perform a straightforward analysis of the thermal properties of TiOCl and we will show that we arrive at a rather consistent description despite the large uncertainties mentioned above.

Figure 2 shows the heat capacity for the complete temperature regime investigated, plotted as C/T vs T . Assuming a $S=1/2$ spin chain, the contribution of the spin chain for $T > 67 \text{ K}$ is modeled by a Bonner-Fisher type of behavior,²⁰ taking into account an exchange coupling $J=660 \text{ K}$. For the low-temperature regime, i.e., below the spin-Peierls transition at $T_{c1}=67 \text{ K}$, the expected exponential decrease of the spin part of the heat capacity is simulated by a BCS-like mean-field treatment²¹ with a temperature-dependent gap, $2\Delta_0 = 3.5k_B T_{c1}$, and, at T_{c1} , a heat capacity jump of 1.43 times the contribution of the spin chain, as it was proposed for canonical spin-Peierls systems.¹ Using this approach we

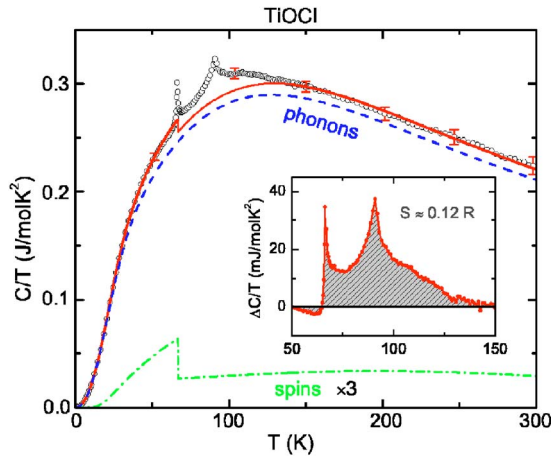


FIG. 2. (Color online) Heat capacity of TiOCl plotted as C/T vs T . The $S=1/2$ contribution including a mean-field spin-Peierls transition as described in the text is indicated as a dash-dotted line. For representation purposes the calculated values have been multiplied by a factor of 3. The fit to the phonon-derived specific heat (see text) is indicated as a dashed line. The sum of both contributions is drawn as a solid line and represents the best fit to the experimental results. The inset shows the difference between calculated and measured heat capacities in a limited temperature regime.

can calculate the spin-derived heat capacity without any free parameter. The result (for representation multiplied by a factor of 3) is shown as a dash-dotted line in Fig. 2. We are aware that this can only be a very rough analysis, specifically having in mind that the actual gap in TiOCl seems to be much larger and has recently been determined as $2\Delta \approx 10, \dots, 15k_B T_{c1,c2}$ by NMR experiments¹² and that the transition actually is of first order. The disregard of these experimental facts gives an underestimation of the jump height of the magnetic specific heat at the spin-Peierls transition and a too broad decay below, leading indeed to observable differences between the measured data and our calculation closely below T_{c1} . However, the overall entropy balance is not affected by these shortcomings of our simple model. The total magnetic entropy at high temperatures sums up to $R \ln 2$ as expected for a spin $1/2$ system.

The phonon system has been fitted assuming one Debye- and two Einstein-type contributions, yielding a total of five free parameters, namely, the mean Debye (Θ_D) and two Einstein temperatures ($\Theta_{E_{1,2}}$), and the ratio of Debye to Einstein modes $R_{D/E}$, as well as the ratio between the Einstein modes R_{E_1/E_2} . The number of degrees of freedom (N_f), which of course should be nine per formula unit of TiOCl, was kept fixed. The experimentally determined heat-capacity values for $2 \text{ K} < T < 65 \text{ K}$ and $130 \text{ K} < T < 300 \text{ K}$ have been used for the fit of the heat capacity. For the fitting procedure we included the spin contributions which have been calculated parameter free as outlined above. The total heat capacity, spin, and phonon contributions are shown as a solid line in Fig. 2. The lattice-derived heat capacity is indicated as a dashed line. Despite this oversimplified model we arrive at an astonishingly good description of the heat capacity over the complete temperature range. The parameters as deter-

mined by the best fit seem to be realistic: The characteristic temperatures, $\Theta_D=188 \text{ K}$, $\Theta_{E_1}=352 \text{ K}$, and $\Theta_{E_2}=614 \text{ K}$, with the ratios $R_{D/E}=0.30$ and $R_{E_1/E_2}=0.51$ determining the relative weight of Debye and Einstein modes, are reliable keeping in mind that the optical-phonon modes in TiOCl range from approximately 100 to 700 K with dominant modes close to our values for $\Theta_{E_{1,2}}$ (Refs. 10 and 11). The small discrepancy of the Debye temperature obtained from this overall fit to $C(T)$, compared to the value derived from the low-temperature heat capacity only, can be explained by the presence of relatively low-lying optical modes.

Comparing the model heat capacity to the measured one in Fig. 2 we find very good agreement for the smooth temperature evolution for low ($T < T_{c1}$) and high ($T > T_{c2}$) temperatures. As clearly seen, the main deviations arise in the temperature region between the two phase transitions. The good agreement concerning the smooth part of the heat capacity may seem surprising in light of our simplified model. On the other hand, the phonon part of our $C(T)$ model is reasonably close to a realistic description involving the true phonon spectrum and the spin part of the heat capacity bears only a small weight. Thus, we believe that our model yields a reliable estimate of the regular part of the specific heat, allowing us to separate out the anomalous contribution due to the phase transitions at T_{c1} and T_{c2} . The inset of Fig. 2 shows this extra heat capacity in a limited temperature range from 50 to 150 K. The integral over this region gives an estimate of the entropy ΔS being released when going through both transitions. ΔS is of the order of $0.12 R$ ($\pm 0.02 R$), vanishingly small compared to $R \ln 2$ expected for a spin $S=1/2$ system or an orbital doubly degenerate state. Orbital entropy contributions of this order of magnitude previously have been monitored for e_g systems.^{22,23} In the present case even a $R \ln 3$ contribution could be expected for an order-disorder transition of the degenerate orbital t_{2g} triplet. From this we can conclude that, in addition to the considered phonon and magnetic contributions, at least no generic orbital-order scenario can be attributed to the phase transitions at T_{c1} and T_{c2} . The narrow peak at T_{c1} corresponds to the latent heat released at the phase transition where according to magnetic measurements spin dimerization appears. The larger fraction of the entropy is covered under the phase transition at T_{c2} extending up to 135 K, exactly the temperature where in NMR experiments the fluctuation effects and the opening of a pseudogap have been detected.¹² In this sense our results would also be compatible with observations of Raman scattering¹¹ and with the results of density-functional calculations, suggesting that TiOCl may be subject to orbital fluctuations.¹⁵ Unfortunately, our specific-heat data do not allow us to decide on the precise microscopic nature of the fluctuations (spin-Peierls or orbital). On the other hand, very recently Rückamp and co-workers¹⁴ concluded from cluster calculations in combination with optical measurements that the orbital ground state is determined by a crystal-field splitting in the order of $\approx 0.3 \text{ eV}$ stabilizing the occupation of the d_{xy} levels²⁴ and thus strongly suppressing orbital fluctuations in the examined temperature range. This reasoning is experimentally confirmed by recent polarization-dependent photoemission

measurements.²⁵ Hence the phase above T_{c1} has to be characterized not by orbital but rather by spin-Peierls fluctuations, retaining some sort of incommensurate or short-range order and thereby delaying the release of the full entropy towards higher temperatures.

IV. CONCLUSIONS

Summarizing, we have measured the heat capacity of TiOCl for temperatures $2\text{ K} < T < 300\text{ K}$ and magnetic fields up to 5 T. We observed two anomalies at $T_{c1}=91\text{ K}$ and $T_{c2}=67\text{ K}$ corresponding to two subsequent phase transitions. The total heat capacity can satisfactorily be explained describing the phonon spectrum with Debye and Einstein modes and the magnetic excitations by a Bonner-Fisher-type heat capacity for $T > T_{c1}$ and the opening of a spin gap below. The phase transition at 67 K, where strong spin dimerization sets in, reveals significant hysteresis effects and hence is of first order. The phase transition at T_{c2} does not

show thermal hysteresis but carries the major part of the transition entropy. However, this entropy contribution is vanishingly small compared to the expectation for any additional conventional order-disorder transition, indicating that the regarded temperature regime might be simply dominated by fluctuations due to a complex spin-Peierls scenario. At low temperatures and zero external fields the heat capacity can satisfactorily be described by taking a phonon-derived T^3 term into account only. No indication of contributions of low-energy excitations can be detected.

ACKNOWLEDGMENTS

We want to thank R. Valenti, J. Deisenhofer, H.-A. Krug von Nidda, and R. Rückamp for helpful discussions. This work was partly supported by the Bundesministerium für Bildung und Forschung (BMBF) via Grant No. VDI/EKM 13N6917-A and by the Deutsche Forschungsgemeinschaft (Sonderforschungsbereich 484 in Augsburg and project CL 124/3-3).

*Present address: II. Physikalisches Institut, Universität zu Köln, D-50937 Köln, Germany.

†Permanent address: Experimentelle Physik 4, Universität Würzburg, D-97074 Würzburg, Germany.

¹J. W. Bray, H. R. Hart, Jr., L. V. Interrante, I. S. Jacobs, J. S. Kasper, G. D. Watkins, S. H. Wee, and J. C. Bonner, *Phys. Rev. Lett.* **35**, 744 (1975).

²M. Hase, I. Terasaki, and K. Uchinokura, *Phys. Rev. Lett.* **70**, 3651 (1993).

³M. Isobe and Y. Ueda, *J. Phys. Soc. Jpn.* **65**, 1178 (1996).

⁴J. Lüdecke, A. Jobst, S. van Smaalen, E. Morre, C. Geibel, and H.-G. Krane, *Phys. Rev. Lett.* **82**, 3633 (1999); M. Lohmann, H.-A. Krug von Nidda, M. V. Eremin, A. Loidl, G. Obermeier, and S. Horn, *ibid.* **85**, 1742 (2000).

⁵R. J. Beynon and J. A. Wilson, *J. Phys.: Condens. Matter* **5**, 1983 (1993).

⁶A. Seidel, C. A. Marianetti, F. C. Chou, G. Ceder, and P. A. Lee, *Phys. Rev. B* **67**, 020405(R) (2003).

⁷C. Friedel and J. Guerin, *Ann. Chim. Phys.* **8**, 36 (1876).

⁸H. Schäfer, F. Wartenpfehl, and E. Weise, *Z. Anorg. Allg. Chem.* **295**, 268 (1958).

⁹V. Kataev, J. Baier, A. Möller, L. Jongen, G. Meyer, and A. Freimuth, *Phys. Rev. B* **68**, 140405(R) (2003).

¹⁰G. Caimi, L. Degiorgi, N. N. Kovaleva, P. Lemmens, and F. C. Chou, *Phys. Rev. B* **69**, 125108 (2004).

¹¹P. Lemmens, K. Y. Choi, G. Caimi, L. Degiorgi, N. N. Kovaleva, A. Seidel, and F. C. Chou, *Phys. Rev. B* **70**, 134429 (2004).

¹²T. Imai and F. C. Chou, *cond-mat/0301425* (unpublished).

¹³M. Shaz, S. van Smaalen, L. Palatinus, M. Hoinkis, M. Klemm, S. Horn, and R. Claessen, *Phys. Rev. B* **71**, 100405(R) (2005).

¹⁴R. Rückamp, J. Baier, M. Kriener, M. W. Haverkort, T. Lorenz, G. S. Uhrig, L. Jongen, A. Möller, G. Meyer, and M. Grüninger, *cond-mat/0503409* (unpublished).

¹⁵T. Saha-Dasgupta, R. Valenti, H. Rosner, and C. Gros, *Europhys. Lett.* **67**, 63 (2004).

¹⁶L. Craco, M. S. Laad, and E. Müller-Hartmann, *cond-mat/0410472* (unpublished).

¹⁷T. Saha-Dasgupta, A. Lichtenstein, and R. Valenti, *Phys. Rev. B* **71**, 153108 (2005).

¹⁸J. C. Lashley, M. F. Hundley, A. Migliori, J. L. Sarrao, P. G. Pagliuso, T. W. Darling, M. Jaime, J. C. Cooley, W. L. Hults, L. Morales, D. J. Thoma, J. L. Smith, J. Boerio-Goates, B. F. Woodfield, G. R. Stewart, R. A. Fisher, and N. E. Phillips, *Cryogenics* **43**, 369 (2003).

¹⁹J. C. Lasjaunias, J. P. Brison, P. Monceau, D. Staresinic, K. Biljakovic, C. Carcel, and J. M. Fabre, *J. Phys.: Condens. Matter* **14**, 837 (2002).

²⁰J. C. Bonner and M. E. Fisher, *Phys. Rev.* **135**, A640 (1964).

²¹B. Mühlshlegel, *Z. Phys.* **155**, 313 (1959).

²²V. Fritsch, J. Hemberger, N. Büttgen, E.-W. Scheidt, H.-A. Krug von Nidda, A. Loidl, and V. Tsurkan, *Phys. Rev. Lett.* **92**, 116401 (2004).

²³R. Fichtl, V. Tsurkan, P. Lunkenheimer, J. Hemberger, V. Fritsch, H.-A. Krug von Nidda, E.-W. Scheidt, and A. Loidl, *Phys. Rev. Lett.* **94**, 027601 (2005).

²⁴In literature the regarded orbital states are denoted either as d_{xy} or $d_{x^2-y^2}$, depending on the choice of the local coordinate system, which may be either the crystallographic axis or the TiO_4Cl_2 octahedron.

²⁵M. Hoinkis *et al.*, *cond-mat/0506203* (unpublished).